LAPORAN PENELITIAN

"WIND WAVE MODELING IN NATUNA SEA: A COMPARISON AMONG SWAN, SEAFINE, AND ERA-INTERIM"

Dr. Yati Muliati

INSTITUT TEKNOLOGI NASIONAL
BANDUNG - 2019

WIND WAVE MODELING IN NATUNA SEA: A COMPARISON AMONG SWAN, SEAFINE, AND ERA-INTERIM

Article *in* International Journal of GEOMATE · February 2019

DOI: 10.21660/2019.54.93272

CITATIONS
6

READS
464

5 authors, including:

Widodo S. Pranowo
Ministry of Marine Affairs & Fisheries Republic of Indonesia
104 PUBLICATIONS **966** CITATIONS
SEE PROFILE

Andojo Wurjanto
Bandung Institute of Technology
36 PUBLICATIONS **426** CITATIONS
SEE PROFILE

Ricky Tawekal
Bandung Institute of Technology
22 PUBLICATIONS **55** CITATIONS
SEE PROFILE

Yati Muliati
Institut Teknologi Nasional
7 PUBLICATIONS **17** CITATIONS
SEE PROFILE

International Journal of GEOMATE, Feb., 2019 Vol.16, Issue 54, pp.176 - 184
Geotec., Const. Mat. & Env., DOI: https://doi.org/10.21660/2019.54.93272
ISSN: 2186-2982 (Print), 2186-2990 (Online), Japan

WIND WAVE MODELING IN NATUNA SEA: A COMPARISON AMONG SWAN, SEAFINE, AND ERA-INTERIM

*Yati Muliati[1,2], Ricky Lukman Tawekal[1], Andojo Wurjanto[1], Jaya Kelvin[3], and Widodo Setiyo Pranowo[3,4]

[1]Faculty of Civil and Environmental Engineering, Institut Teknologi Bandung, Indonesia,
[2]Faculty of Civil Engineering and Planning, Institut Teknologi Nasional (Itenas) Bandung, Indonesia,
[3]Marine Research Center, Indonesian Ministry of Marine Affairs & Fisheries,
[4]Department of Tech. Hydrography, Indonesian Naval Postgraduate School (STTAL).

*Corresponding Author, Received: 30 Oct. 2018, Revised: 10 Dec. 2018, Accepted: 31 Dec. 2018

ABSTRACT: This research was conducted to verify the wave height hindcasting in Natuna Sea using the SWAN (Simulating Wave Near-shore) model, which is compared with the results of hindcasting from SEAFINE (SEAMOS South Fine Grid Hindcast) and ERA-Interim. This is expected to support research on wave characteristics based on wave forecasting for 10 years in the seas among Java, Sumatera, and Kalimantan. So the purpose of this research was to test the SWAN modeling of existing models. If the results of the comparison show similar wave distribution patterns, then the settings in the SWAN model can be used for SWAN modeling in Indonesia. The SWAN model is run with the third-generation mode (GEN3), which allow wind input, quadruplet and triad interactions, whitecapping, and breaking. Comparison of hindcasting results among SWAN, SEAFINE, and ERA-Interim produces a similar wave distribution pattern, with a good correlation coefficient for 5 stations (R=0.78-0.84). The SWAN model produces the lowest Hs estimates, while the SEAFINE model produces the highest Hs of all stations. Significant wave height (Hs) 100 years return period for all stations in Natuna Sea from SWAN is 2.97-3.37 m, ERA-Interim 4.01-4.13 m, and SEAFINE 5.24-5.67 m. The setting up of wave hindcast in this research will be helpful for improving the level of sea wave hindcast in the seas among Java, Sumatera, and Kalimantan.

Keywords: Wind-wave model, SWAN, SEAFINE, Hindcast, Significant Wave Height

1. INTRODUCTION

For about 50 years, wind-driven numerical wave prediction models have proven useful for ship routing, offshore technology, onshore and offshore structure, and also for climate research. Since the pioneering model by Gelci et al in 1957, many wave models have been developed in which the complicated nature of wave generation, propagation and decay has been described [1]. Up to the late 1980's many models developed, using simple nonlinear interaction approximations and/or assumptions on the spectral shape (first and second generation models). Development of the third generation models (3G) started in 1993. This model parameterizes all physical processes explicitly, without imposing spectral shapes or energy levels [2]. One of these 3G models is SWAN. This numerical model is chosen because it is suitable for shallow water [3] and SWAN has been already successfully used to model waves in coastal regions [3-14].

The SEAFINE is a joint industry project (JIP) administered by Oceanweather, Inc. (OWI), where SEAMOS is South East Asia Meteorological and Oceanographic Hindcast Study. This study is to help design offshore structures and plan offshore operations in the general area of the South China Sea (SCS) and immediately contiguous basins. Access to SEAFINE is governed by the terms of a JIP Agreement executed between OWI and each SEAFINE Participant [15].

The main purpose of developing such numerical model is to understand the dynamic of wave processes and the wave climate which then could be used to reduce the impact of extreme events. In the previous study by Muliati et al. [3], the development of a regional wave model in Java Sea by using the SWAN model was one of the examples. However, a further question arises by looking at the design of the study area and validation point. Even though the model has a good agreement with the validation point at Jepara, it might not be representative of the whole region with that size. Therefore, in this study, the focus is to assess the quality of hindcasting result with longer period by comparing with another model that is available in Natuna Sea, which is SEAFINE model [15], and to determine the limitations of Muliati et al. [3] regional model. By doing so, future improvement of the regional model in the Java Sea is expected.

In addition, this study includes the ERA-Interim model output to the comparison. The ERA-Interim is a global atmospheric reanalysis from 1979, continuously updated in real time, and can be

downloaded from the ECMWF (European Centre for Medium-Range Weather Forecasts) Public Datasets web interface [16].

This study is expected to support wave characteristic research based on wave forecasting for 10 years in the waters between Java, Sumatera, and Kalimantan. In the initial plan, this research will use altimetry data, but wave height validation from altimetry data to the results of wave gauge measurement in Indonesia shows that significant wave height from altimetry data is less accurate for use [17].

2. NUMERICAL SCHEMES

Waves generated by wind are one of the important parameters in coastal and ocean engineering. Random sea level waves are one of the most complex phenomena. The characteristics of ocean waves can be formulated based on the results of wave measurements, numerical simulations, physical models and analytical solutions. Each method has its own advantages and disadvantages. But now, numerical models emerge as one of the most powerful tools for studying surface water waves [18]. The numerical wave models express the physical concepts of the phenomena [19]. Performance of the numerical wave model depends on how best the phenomena are expressed into the numerical schemes, so that more accurate wave parameters could be estimated [19]. The numerical wave models developed were based on energy balance equation with various components of the source function as inputs [19].

All information about the sea surface is contained in the wave variance spectrum or energy density $E(\sigma,\theta)$, distributing wave energy over (radian) frequencies σ (as observed in a frame of reference moving with current velocity) and propagation directions θ (the direction normal to the wave crest of each spectral component). Usually, wave models determine the evolution of the action density $N(x,t;\sigma,\theta)$ in space x and time t. The action density is defined as $N=E/\sigma$ and is conserved during propagation in the presence of ambient current, whereas energy density E is not. It is assumed that the ambient current is uniform with respect to the vertical coordinate and is denoted as U [20].

The evolution of the action density N is governed by the action balance equation, which reads [21]:

$$\frac{\partial N}{\partial t} + \nabla_x\left[\left(c_g + U\right)N\right] + \frac{\partial c_\sigma N}{\partial \sigma} + \frac{\partial c_\theta}{\partial \theta} = \frac{S_{tot}}{\sigma} \quad (1)$$

The left-hand side is the kinematic part of this equation. The second term denotes the propagation of wave energy in two-dimensional geographical x-space, with the group velocity $c_g = \partial\sigma/\partial k$ following from the dispersion relation $\sigma^2 = g|k| \tanh(|k|d)$ where k is the wave number vector and d the water depth. The third term represents the effect of shifting of the radian frequency due to variations in depth and mean currents. The fourth term represents depth-induced and current-induced refraction. The quantities c_σ and c_θ are the propagation velocities in spectral space (σ,θ). The right-hand side contains S_{tot}, which is the source/sink term that represents all physical processes which generate, dissipate, or redistribute wave energy. They are defined for energy density $E(\sigma,\theta)$. The second term in Eq. (1) can be recast in Cartesian, spherical or curvilinear coordinates. For small-scale applications, the spectral action balance equation may be expressed in Cartesian coordinates as given by [20]:

$$\frac{\partial N}{\partial t} + \frac{\partial c_x N}{\partial x} + \frac{\partial c_y N}{\partial y} + \frac{\partial c_\sigma N}{\partial \sigma} + \frac{\partial c_\theta N}{\partial \theta} = \frac{S_{tot}}{\sigma} \quad (2)$$

with

$$c_x = c_{g,x} + U_x \ , \quad c_y = c_{g,y} + U_y \quad (3)$$

With respect to applications at shelf sea or oceanic scales the action balance equation may be recast in spherical coordinates as follows [20]:

$$\frac{\partial N}{\partial t} + \frac{\partial c_\lambda N}{\partial \lambda} + cos^{-1}\varphi \frac{\partial c_\varphi cos\varphi N}{\partial \varphi} + \frac{\partial c_\sigma N}{\partial \sigma} + \frac{\partial c_\theta N}{\partial \theta} = \frac{S_{tot}}{\sigma} \quad (4)$$

with longitude λ and latitude φ [20].

In shallow water, six processes contribute to S_{tot}:

$$S_{tot} = S_{in} + S_{nl3} + S_{nl4} + S_{ds,w} + S_{ds,b} + S_{ds,br} \quad (5)$$

These terms denote, respectively, wave growth by the wind, nonlinear transfer of wave energy through three-wave and four-wave interactions and wave decay due to whitecapping, bottom friction and depth-induced wave breaking [20].

There are some options in SWAN regarding the model set-up which pertains to the type and/or parameterization of the formulations used for the source terms in Eq.(5). The user can choose between three different formulations for S_{in}, which accounts for the linear and exponential growth of waves due to wind [13].

Wind energy to waves is commonly described as the sum of linear and exponential growth. There are two wind growth models in SWAN that are available for us. Both expressions of wind growth model of them share the following form (Eq.(6)) and the same linear growth (Eq.(7)), while the exponential growth term is different.

$$S_{in}(\sigma,\theta) = A + BxE(\sigma,\theta) \quad (6)$$

In which *A* describes linear growth and *BxE* exponential growth [11].

Linear growth by wind:

$$A = \frac{\alpha}{g^2 2\pi}[U_* \max(0, \cos(\theta - \theta_w))]^4 H \quad (7)$$

with

$$H = \exp(-(\sigma/\sigma^*_{PM})^{-4}) \quad \text{and} \quad \sigma^*_{PM} = \frac{0.13g}{28U_*} 2\pi \quad (8)$$

Exponential growth:

a. Expression from [22]:

$$B = \max[0, 0.25 \frac{\rho_a}{\rho_w}\left(28 \frac{U_*}{C_{ph}} \cos(\theta - \theta_w) - 1\right)]\sigma \quad (9)$$

in which U_* is friction velocity, θ_w is wind direction, C_{ph} is the phase speed and ρ_a and ρ_w are the density of air and water, respectively.

b. Expression from [23]:

$$B = \beta \frac{\rho_a}{\rho_w}(\frac{U_*}{C_{ph}})^2 (\max(0, \cos(\theta - \theta_w)))^2 \sigma \quad (10)$$

where β is the Miles"constant".

The dissipation term of wave energy is represented by the summation of three different contributions: white-capping $S_{ds,w}$, bottom friction $S_{ds,b}$ and depth-induced breaking $S_{ds,br}$ [20].

3. MATERIALS AND METHODS

3.1 Data

The scarcity of time series oceanographic datasets, especially the observational wave data, is one of the challenges to developing the ocean model in Indonesia [3].

The bathymetry data is obtained from the General Bathymetric Chart of the Oceans (GEBCO) with a spatial resolution of 30 arc-sec (~1 km). There is no available local bathymetry dataset to cover the Natuna Sea. Therefore, GEBCO data are applied to all model domains. The only forcing included in this wave model is the wind. It is obtained from the ECMWF with a spatial resolution of 0.125 degrees (~13.75 km) and 6-hour temporal resolution.

The significant wave height (Hs) output from SEAFINE and from the ECMWF Re-analysis (ERA)-Interim reanalysis are used in a comparison to the model.

3.2 Model Domain

The SWAN model provides nesting application to the parent grid. Hence, there are two model domains, the Java Sea (JS) domain as the parent grid and Natuna Sea (NS) domain as the child/nested grid (Fig. 1). The JS domain extends from Aceh to Bali that includes two marginal seas, i.e. the South China Sea and the Java Sea, while the NS domain covers the Natuna Sea particularly with the existence of offshore oil rigs (104.472ºE -107.498ºE and 4.956ºS - 3.572ºS). The JS and NS domains have 1/8 degree and 1/96 grid resolutions with the total of 176x120 and 44x48 grid-cells, respectively.

The bathymetry in the region is relatively shallow (<100 m), with the presence of narrow straits (e.g. Malacca Strait) and small islands that add more complexity to the model domain (Fig. 1).

3.3 Model Setup

Modeling design of SWAN for this article is adopted from Muliati et al. [3] since has been validated in certain levels. The non-stationary 2D wave model within SWAN is simulated with a 1-hour interval from 1 January 2007 to 30 June 2015 and use 5 virtual stations for results comparisons. The location of stations (wave hindcasting) and different values of depth in model SWAN and SEAFINE are presented in Table 1.

The frequency range is set at 0.3-1.1 Hz and divided linearly into 38 frequencies. The number of directional bins is set for 72 dues to the physical characteristics of the study areas, such as the geographical conditions, bathymetry gradients, and global and local wind effects [24]. In addition, the first order, backward space, backward time (BSBT) numerical scheme are employed for both model domains with three maximum number of iterations and 98% percentage of accuracy for the wet/dry condition.

The same physics setup is applied to both domains. GEN3 wave model with Komen linear growth formulation and the white capping default configurations were used [22]. Further, the triad and quad wave-wave interaction, as well as breaking and diffraction processes are activated by using the default configurations [20]. For bed friction, the dissipation coefficients (*Cb*) was 0.019 as suggested for the region with smooth sediment characteristic, while the default value is 0.038 [20]. Finally, the model is simulated in parallel computing with openMP to reduce computation times.

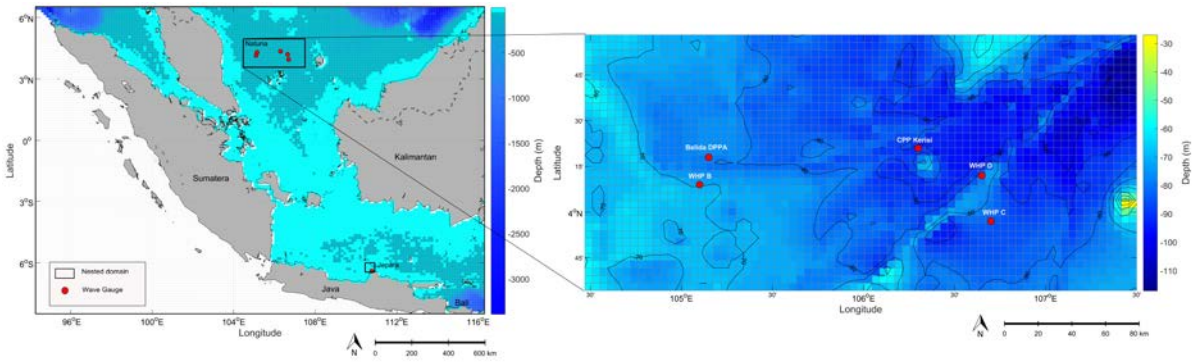

Fig.1 Model domain; (left) regional domain of the Java Sea and (right) nested-domain of Natuna Sea. The nested-domain of Jepara is used for validation as described in Muliati et al. (2018) [3]. Red dots represent the location of wave hindcasting from SEAFINE.

Table 1 The location of wave hindcasting and different values of depth in both models

Stations	Lon (°)	Lat (°)	Depth (m)	
			SWAN	SEA FINE
Belida DPPA	105.15	4.30	78.4	67.0
CPP Kerisi	106.30	4.35	87.5	80.5
WHP B	105.10	4.15	70.5	67
WHP C	106.70	3.95	84.5	76
WHP D	106.65	4.20	76.2	87

3.4 Extreme Value Analysis

Extreme value analysis (EVA) method is applied to be observed or modeled extreme wave heights and allowed the quantification of return periods (or return levels) that are longer than the records, which is 8.5 years of hindcast outputs. One of the simplest techniques used here is the Gumbel distribution analysis. The time series of annual maxima was derived from the model output. Finally, the Gumbel distributions were fitted to the annual maxima at each station. The maximum range of return periods is 100 years as in general, simulations are carried out for planning [25]. This is more than four times of available data, which is not recommended for statistical accuracy reasons [26]. However, to be useful for broad-scale impact and adaptation analyses, such low-probability/high impact events are considered due to the application of this study to the offshore oil rig structures.

4. RESULTS AND DISCUSSION

4.1 Model Comparison

The three models are compared and the pattern is aligned very well between all models (Fig 2), even each station has a similar pattern throughout the year due to the small-size domain and less-complex bathymetry.

SWAN model is under the estimation of the other two models, particularly during the wet season (west monsoon), i.e. Nov-Feb. This is due to the arrangement of domains in the SEAFINE and ERA-Interim models that are larger than the domains in SWAN, so the SEAFINE and ERA-Interim models will be able to generate higher swell waves over long distances.

The SEAFINE model produces the highest estimated value of Hs at all stations. This relates to the use of SEAFINE for offshore structure design and offshore operations planning so that the parameters in the forecast make a higher level of security for planning. It is different from the ERA-Interim which is used for public purposes by meteorological offices in Europe and other countries.

The correlations of Hs is calculated from the longer time series, namely data from January 2007 to June 2015. The correlation analysis of Hs-SWAN with Hs-ERA-Interim results in a correlation coefficient of R1 ranging from 0.83 to 0.84, while Hs-SWAN with Hs-SEAFINE produces R2 correlation coefficients between 0.78-0.81. All correlation coefficients show a strong relationship or suitability between each analysis result.

These three hindcasting models are suitable for Indonesian conditions. Referring to the previous paper [3], the SWAN model is closest to the actual wave event. However, the SEAFINE and ERA-Interim hindcasting will be safer if used in planning offshore structures.

The review of wave numerical modeling by Thomas and Dwarakish [19] states the following conclusions. Comparison of wave models showed that fine grid models are more suitable in the coastal region due to the varying bathymetry while in deep water coarser grid also produces accurate results with a less computational period.

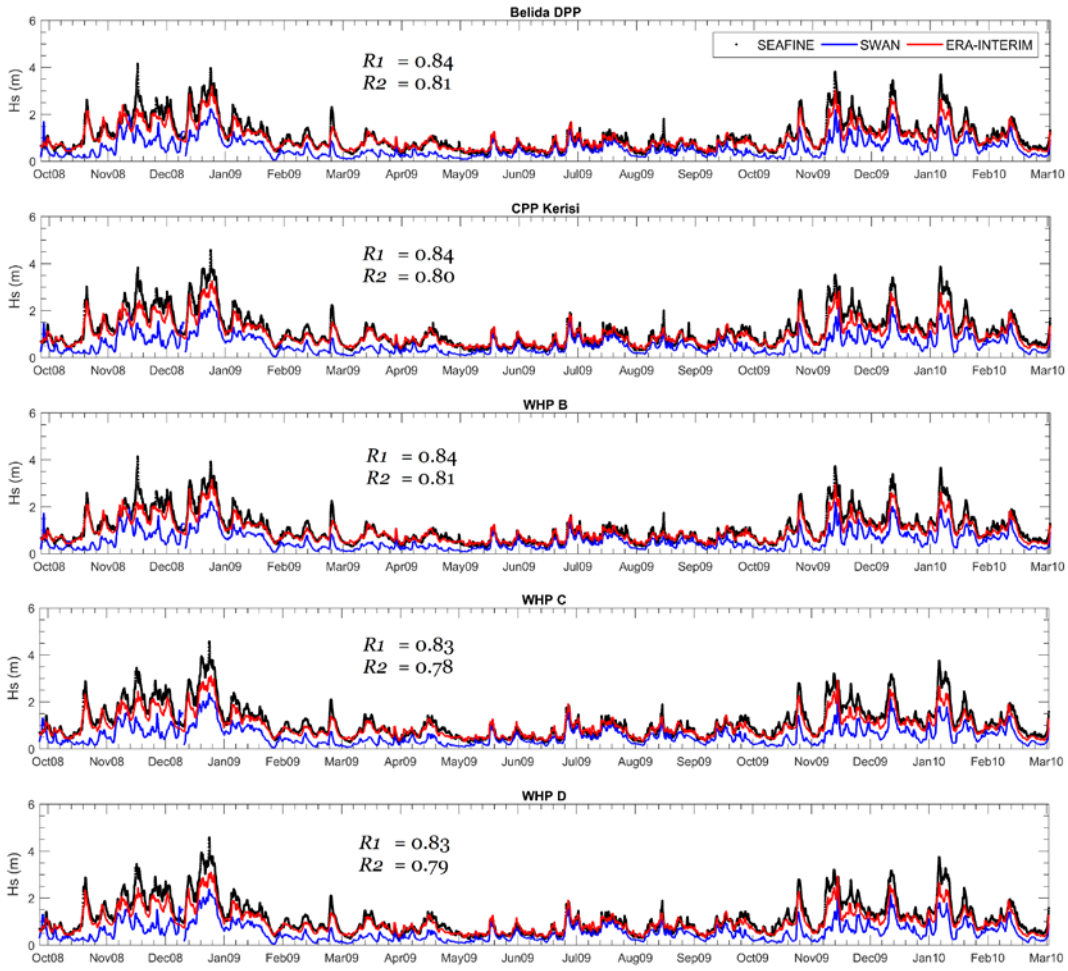

Fig. 2 Time series of Hs in each station from outputs of three different models, i.e. SWAN (blue line), ERA-Interim (red line), and SEAFINE (black points). The correlations are calculated from a longer time series (Jan 2007-Jun 2015). R1 is with ERA-Interim, while R2 is with SEAFINE.

The major input for the numerical model is wind data and the inaccuracy of wind data results in the discrepancies of model results [19].

Steps like data assimilation have been taken to improve the wind data and thus to increase the accuracy of the numerical model. Also by error forecasting, the accuracy of the numerical models can be increased [19].

Wind patterns outputs from SWAN and SEAFINE models are in agreement (Fig. 3). However, similar to the Hs comparison, SWAN model has underestimated the wind speed, and thus generate lower Hs values compared to SEAFINE Hs outputs.

Since both models have similar patterns, apart from the magnitude, the outputs from the SWAN model are transformed to fit with the SEAFINE model outputs using linear transformation. The result shows a higher agreement in terms of reaching the maximum significant wave height (Fig. 4). By average, the different Hs outputs produced from SWAN and SEAFINE is by factor 1.45. The number is quite high considering many extreme events occurred in this region and the SWAN model could not perform well during those events. The other probable reasons are the quality of wind data as well as the bathymetry.

The SWAN model generated in this study is proven to have a bigger error when it comes to the region far away from validation point. Although, this conclusion should be confirmed by doing further studies with more validation points and increase the time range as well. However, it is noteworthy that the wave boundary condition could play a significant role in the model by increasing the probability of generating a higher swell to the small model domain.

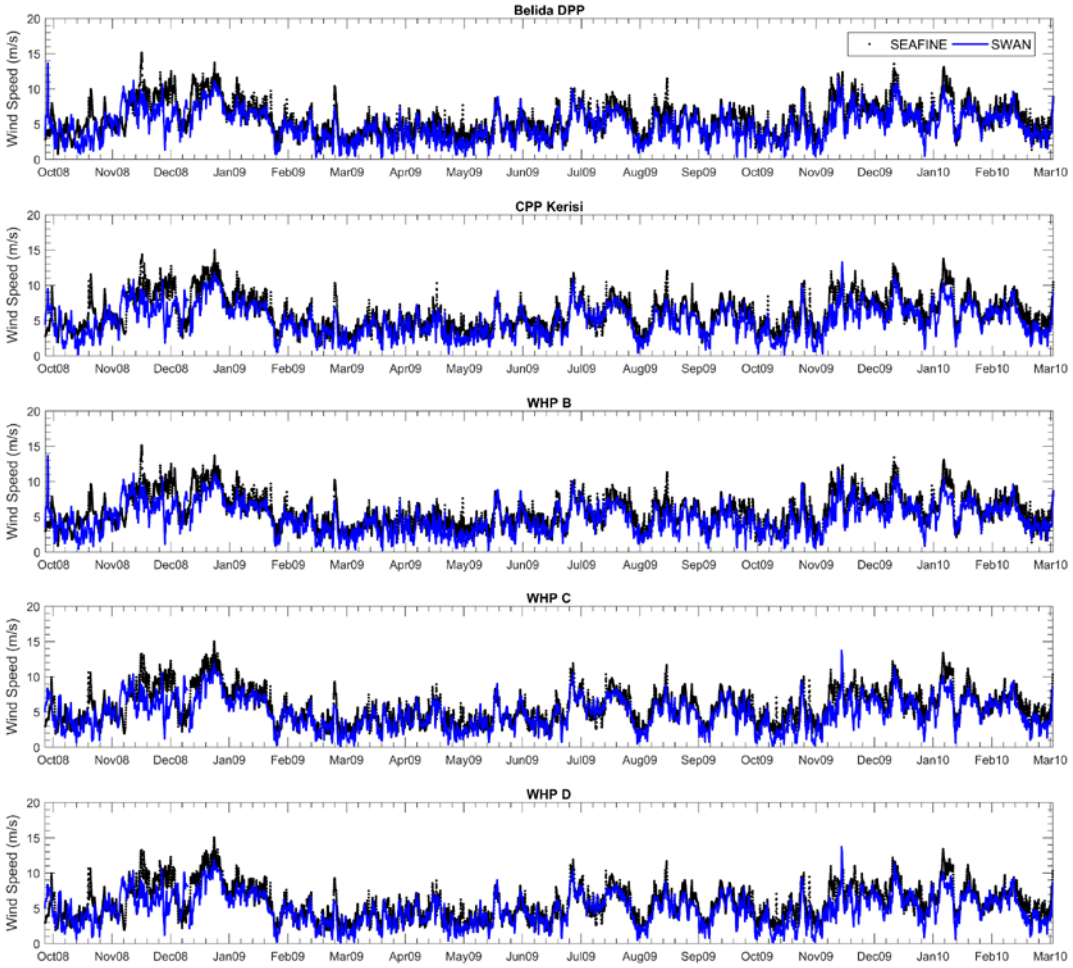

Fig. 3 Time series of wind speed in each station from outputs of SWAN model (blue line) and SEAFINE model (black points).

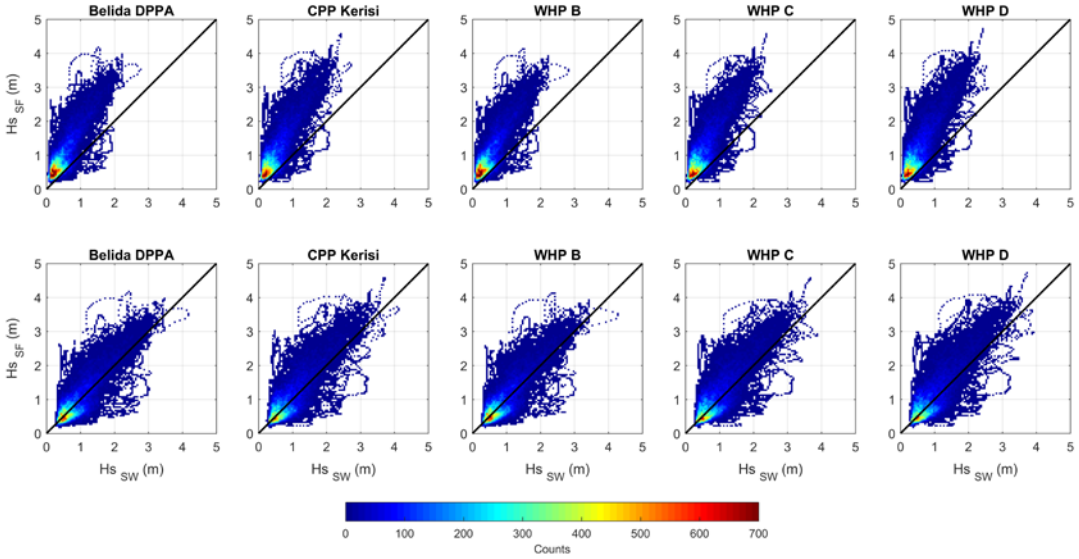

Fig. 4 Significant wave height (Hs) comparison between SWAN (SW) and SEAFINE (SF) models. Results in the top layer are before linear-fitting transformation, while the bottom layer shows results after the transformation.

4.2 Wave Climate

Eight and a half years of hindcasting for Natuna Sea shows seasonal and interannual variations. The focus of Fig. 5 is to show the seasonal variation, i.e. between maximum Hs in summer and winter. The summer has lower maximum Hs than in the winter. Moreover, the spatial pattern shows opposite hotspot for maximum wave height at Natuna Sea. During summer, higher wave heights are observed in the northern part with higher peak period as well. On the other hand, during winter the higher wave heights shifted to the southern part of the Natuna Sea followed by a higher peak period as well.

The maximum Hs observed in the region is ~3 meter with a 6.4 second peak period. The WHP C site gets the biggest wave height during winter than the other sites meanwhile, Belida DPPA site gets the biggest wave height during summer even though with smaller magnitude compared to during winter season. The maximum wave height in the summer is only reached 2.4 m with the peak period of 6 s.

These results are suitable when compared to Hs forecasting in Natuna Sea by Anggara et.al (2018) [27] where the maximum Hs condition occurs in December, January, and February or in the winter season.

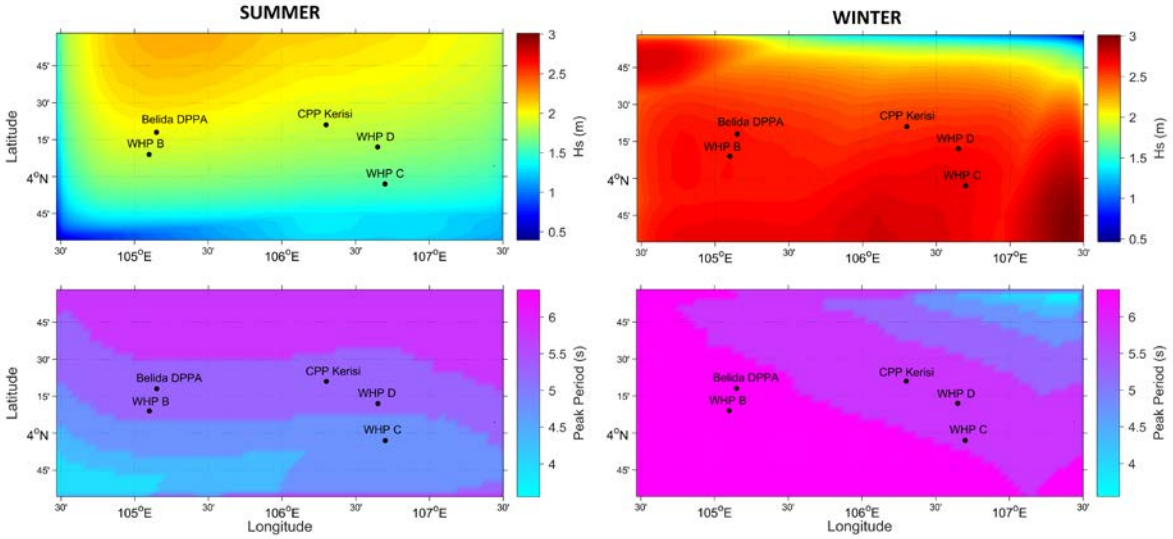

Fig. 5 Seasonal variation of maximum significant wave height (Hs) and peak period (Tp).

Table 2 Return periods (RP) of significant wave height (m) at each station for all the model outputs, i.e SWAN (SW), SEAFINE (SF), and ERA-Interim (EI).

RP (years)	Belida DPPA			CPP Kerisi			WHP B			WHP C			WHP D		
	SW	SF	EI	SW	SF	EI	SW	SF	EI	SW	SF	EI	SW	SF	EI
2	2.09	3.58	2.84	2.24	3.84	3.06	2.08	3.54	2.82	2.21	3.76	2.98	2.26	3.91	3.05
5	2.42	4.04	3.18	2.51	4.27	3.35	2.42	3.99	3.15	2.42	4.21	3.26	2.49	4.38	3.34
10	2.64	4.34	3.41	2.68	4.56	3.54	2.65	4.29	3.37	2.55	4.50	3.44	2.64	4.69	3.52
25	2.91	4.72	3.69	2.91	4.92	3.78	2.94	4.67	3.64	2.72	4.87	3.67	2.84	5.08	3.76
50	3.12	5.00	3.90	3.07	5.19	3.96	3.16	4.96	3.85	2.85	5.14	3.84	2.98	5.38	3.93
100	3.32	5.28	4.11	3.24	5.46	4.13	3.37	5.24	4.05	2.97	5.41	4.01	3.12	5.67	4.11

4.3 Return Period

Table 2 shows the result of extreme value analysis that calculates the 100-years return period. Significant wave height (Hs) 100 years return period for all stations in the Natuna Sea from SWAN is 2.97-3.37 m, ERA-Interim 4.01-4.13 m, and SEAFINE 5.24-5.67 m.

The output from the three models has a different magnitude of wave height prediction. SWAN has the smallest prediction, while SEAFINE has the highest prediction. This is of course caused by the results of forecasting as shown in the form of a time series in Fig. 2, where Hs-SWAN is always lower than Hs-SEAFINE.

5. CONCLUSION

Comparison of hindcasting results among SWAN, SEAFINE, and ERA-Interim produces a similar wave distribution pattern, with a correlation coefficients for 5 stations is 0.78-0.84.

The SWAN model produces the lowest Hs estimates, while the SEAFINE model produces the highest Hs of all stations. This is because the SEAFINE and ERA-Interim models have a larger domain setting than the SWAN model, so both models have the opportunity to produce higher waves from distant sources, and high safety parameters at SEAFINE, given the use of SEAFINE for offshore structure design and offshore operations planning.

The different of Hs outputs produced from SWAN and SEAFINE is by factor 1.45.

Significant wave height (Hs) 100 years return period for all stations in the Natuna Sea from SWAN is 2.97-3.37 m, ERA-Interim 4.01-4.13 m, and SEAFINE 5.24-5.67 m.

The setting up of wave hindcast for Natuna Sea will be helpful for improving the level of shallow sea wave hindcast in the seas among Java, Sumatera, and Kalimantan.

6. ACKNOWLEDGMENTS

The authors would like to thank PT. Bina Rekacipta Utama (Biru), Jakarta, Indonesia for providing SEAFINE wave data and also thank the ECMWF and GEBCO for providing access to wind and bathymetry data, respectively.

Sincere gratitude to Institut Teknologi Nasional (Itenas) Bandung, Indonesia for funding this research and special thanks to the Marine and Coastal Data Laboratory, Indonesian Ministry of Marine Affairs & Fisheries for providing places of simulations.

7. REFERENCES

[1] Massel S.R., Ocean Surface Waves: Their Physics and Prediction, Advanced Series on Ocean Engineering – Volume 11, World Scientific Publishing Co. Pte. Ltd, 1996, pp. 201-224.

[2] Tolman H.L., Balasubramaniyan B., Burroughs L.D., Chalikov D.V., Chao Y.Y., Chen H.S., and Gerald V.M., Development and Implementation of Wind-Generated Ocean Surface Wave Modelsat NCEP, Journals Online of American Meteorological Society, April 2002.

[3] Muliati Y., Tawekal R.L., Wurjanto A., Kelvin J., and Pranowo W.S., Application of SWAN Model for Hindcasting Wave Height in Jepara Coastal Waters, North Java, Indonesia, International Journal of GEOMATE, Vol. 15, Issue 48, 2018, pp. 114-120.

[4] Hamza W., Lusito L., Ligorio F., Tomasicchio G.R., and D'Alessandro F., Wave Climate at Shallow Waters along the Abu Dhabi Coast, Water - MDPI Journal, Vol. 10, Issue 8, 2018, pp. 1-19.

[5] Gorrell L., Raubenheimer B., Elgar S., and Guza R.T., SWAN Predictions of Waves Observed in Shallow Water Onshore of Complex Bathymetry, Coastal Engineering, Vol. 58, 2011, pp. 510-516.

[6] Brown J.M., A Case Study of Combined Wave and Water Levels under Storm Conditions Using WAM and SWAN in a Shallow Water Application, Ocean Modeling, Vol. 35, Issue 3, 2010, pp. 215–229.

[7] Dally W.R., Comparison of a Mid-Shelf Wave Hindcast to ADCP-Measured Directional Spectra and Their Transformation to Shallow Water, Coastal Engineering, Vol. 131, 2018, pp. 12–30.

[8] Xu F., Perrie W., and Solomon S., Shallow Water Dissipation Processes for Wind Waves off the Mackenzie Delta, Atmosphere-Ocean, Vol. 51, 2013, Issue 3, pp. 296–308.

[9] Bottema M., van Vledder G.P., A Ten-year Data Set for Fetch- and Depth-limited Wave Growth. Coastal Engineering, Vol. 56, 2009, Issue 7, pp. 703–725.

[10] Rogers W.E., Kaihatu J.M., Hsu L., Jensen R.E., Dykes J.D., and Holland K.T., Forecasting and Hindcasting Waves with the SWAN Model in the Southern California Bight, Coastal Engineering, Vol. 54, Issue 1, 2007, pp. 1-15

[11] Baoshu Y., Dezhou Y., Application Study of Shallow Water Wave Model (SWAN) in Bohai Sea, Proceedings of The Twelfth OMISAR Workshop on Ocean Models, 2004, pp. 3-1-3-8.

[12] Wolf J., Hargreaves J.C., and Flather R.A., Application of the SWAN Shallow Water Wave

Model to Some U.K. Coastal Sites, Proudman Oceanographic Laboratory Report, No. 57, 51PP, 2000, pp. ii-48.

[13] Atan R., Nash S., and Goggins J., Development of a Nested Local Scale Wave Model for a 1/4 Scale Wave Energy Test Site Using SWAN, Journal of Operational Oceanography, 2017, pp. 1-20.

[14] Gorman R.M., Bryan K.R., and Laing A.K., Wave hindcast for the New Zealand region: Nearshore validation and coastal wave climate, New Zealand Journal of Marine and Freshwater Research, Vol. 37, Issue 3, 2003, pp. 567-588.

[15] SEAFINE, Seamos-South Fine Grid Hindcast A Joint Industry Project Final Report, Oceanweather Inc., November 2008, pp 1-61.

[16] ECMWF, ERA-Interim, www.ecmwf.int/en/forecasts/datasets/archive-datasets/reanalysis-datasets/era-interim, 2018

[17] Muliati Y., Wurjanto A., and Pranowo W.S., Validation of Altimeter Significant Wave Height Using Wave Gauge Measurement in Pacitan Coastal Waters, East Java, Indonesia, International Journal of Advances in Engineering Research, Vol. 12, Issue 4, 2016, pp. 25-33.

[18] Janssen P.A.E.M., Progress in Ocean Wave Forecasting, Journal of Computational Physics, Vol. 227, Issue 7, 2008, pp. 3572-3594.

[19] Thomas J. and Dwarakish G.S., Numerical Wave Modelling – A Review, International Conference on Water Resources Coastal and Ocean Engineering (ICWRCOE 2015), Elsevier B.V., 2015, pp. 443-448.

[20] The SWAN team, SWAN Technical Documentation, Delft University of Technology, 2006, pp. 11–27.

[21] Komen G.J., Cavaleri L., Donelan M., Hasselmann K., Hasselmann S., and P.A.E.M. Janssen, Dynamics and Modelling of Ocean Waves, Cambridge Univ. Press, 1994, pp. 532

[22] Komen G.J., Hasselmann S., and Hasselmann K, On the Existence of a Fully Developed Windsea Spectrum, Journal of Physical Oceanography, 14, 1984, pp. 1271-1285.

[23] Janssen P.A.E.M., Quasi-linear Theory of Wind-wave generation applied to Wave Forecasting, Journal of Physical Oceanography, 21, 1991, pp.1631-1641.

[24] WMO, Guide to wave analysis and forecasting, Second ed, Geneva, Switzerland: Secretariat of the World Meteorological Organization (WMO), 1998.

[25] Romali N.S., Yusop Z., Ismail A.Z., Application of Hec-Ras and Arc Gis for Floodplain Mapping in Segamat Town, Malaysia, International Journal of GEOMATE, Vol. 15, Issue 47, 2018, pp. 7-13.

[26] Pugh D., and Woodworth P., Sea-Level Science: Understanding Tides, Surges, Tsunamis and Mean Sea-Level Changes, Cambridge University Press, 2014, pp. 319-321.

[27] Anggara P.D., Alam T.M., Adrianto D., Pranowo W.S., The Wave Characteristics in Natuna Sea and its Adjacent for Naval Operation Base Purposes, IOP Conference Series: Earth and Environmental Science, 176 012003, 2018, pp. 1-11.